# Breakdown of time-reversal symmetry of photoemission and its inverse in small silicon clusters

Soh Ishii,[1] Kaoru Ohno,[2] Vijay Kumar,[1,3] and Yoshiyuki Kawazoe[1]
[1]*Institute for Materials Research, Tohoku University, Katahira, Sendai 980-8577, Japan*
[2]*Department of Physics, Graduate School of Engineering, Yokohama National University, Tokiwadai, Yokohama 240-8501, Japan*
[3]*Dr. Vijay Kumar Foundation, 45 Bazaar Street, K.K. Nagar (West), Chennai 600 078, India*
(Received 27 March 2003; revised manuscript received 5 September 2003; published 20 November 2003)

Absolute values of the quasiparticle energies of small silicon clusters ($Si_n$, $n=4,5,6$) are determined quite accurately by means of the state-of-the-art *ab initio* calculations in the *GW* approximation, under the all-electron mixed-basis representation. We find that the electron affinity, which is very sensitive to the ionic valence and the cluster geometry, depends strongly on the photoemission process, and that the time-reversal symmetry is completely broken between the photemission and its inverse process. This is due to large structural changes in $Si_5^-$ and $Si_6^-$ as compared to the neutral clusters. When appropriate structural energy changes are taken into account, the time-reversal symmetry is satisfied and all results agree excellently with the preexisting experimental data.

DOI: 10.1103/PhysRevB.68.195412 PACS number(s): 73.22.−f, 31.15.Lc, 32.10.Hq, 71.45.Gm

Silicon clusters have attracted great attention in recent years due to their potential in future miniature devices as well as the desire to take advantage of the widely developed silicon based infrastructure. There are novel phenomena arising due to quantum confinement in clusters such as photoluminescence and electroluminescence that could play an important role in nanoscale electronic and optical devices and in designing materials by the control of the band gap as a function of the cluster size. A proper understanding of the optical gap would require knowledge of the ionization potentials (IP's) and the electron affinities (EA's) that are the most fundamental and important quasiparticle energies. In this paper we investigate them for the small silicon clusters ($Si_n$, $n=4,5,6$) and demonstrate that there is complete breakdown of the time-reversal symmetry between the photoemission and its inverse process due to large structural changes in anion clusters.

The geometrical shapes and the electronic structures of small clusters are quite different from bulk due to the large quantum size effects and have been investigated in detail.[1,2] However, the optical properties have not been fully understood.[3,4] An important fact is that the geometrical shapes and the electronic structures of small clusters could depend strongly on their charge state as has been found for the $Si_5^-$ cluster.[5] In this case large structural relaxations have been obtained as compared to $Si_5$. In such systems the IP and EA depend on the process of experimental measurements, and the time-reversal symmetry is broken between the photoemission and its inverse process. That is, an electron attaching to a neutral cluster emits a small energy photon, while an electron detaching from its anion absorbs a large energy photon. The system would work as a photon energy transformer. The extremum is the case of a very short-time (vertical) process, where the ionic relaxation does not proceed during the reaction. The time-reversal symmetry holds only for a very long-time (adiabatic) process, where the ionic relaxation is complete.

In spite of these interests, no theoretical effort has been devoted so far to this issue of the breakdown of the time-reversal symmetry. The small silicon clusters may offer a prominent example of the systems exhibiting such phenomena. Here we investigate the IP and EA of small silicon clusters by means of the state-of-the-art *ab initio* calculations in the *GW* approximation[6–9] (GWA) on the basis of standard many-body perturbation theory, which can yield reliable estimates of the quasiparticle energies with a modest effort.

In the first part of the present study, we used all-electron GAUSSIAN98 program to optimize the geometry of the small silicon clusters with 6-311+G* basis set and the B3PW91 hybrid exchange-correlation functional in order to obtain good structural data.[10] The resulting geometrical shapes of $Si_n$ and $Si_n^-$ are shown in Figs. 1(a) and 1(b), respectively. The optimized geometry of $Si_4$ has a planar rhombus structure with bond length of 2.30 Å. The most stable structure of

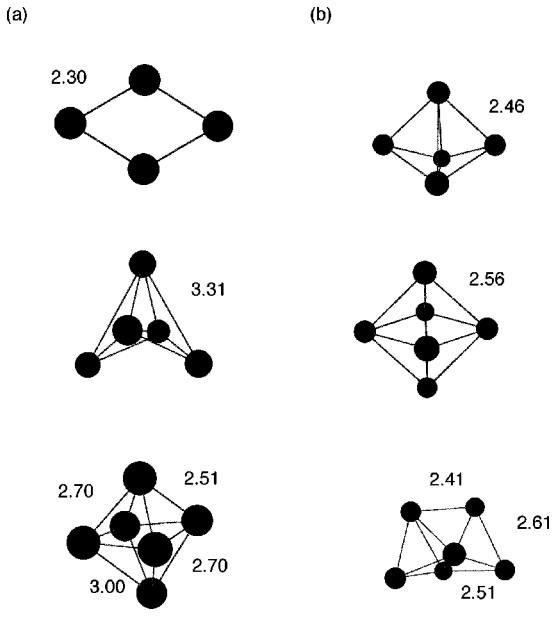


FIG. 1. The geometry of (a) neutral silicon clusters and (b) negatively charged silicon clusters. There are two structures of $Si_6^-$ which are nearly degenerate. One is a bicapped tetrahedron and the other is a distorted octahedron.

 

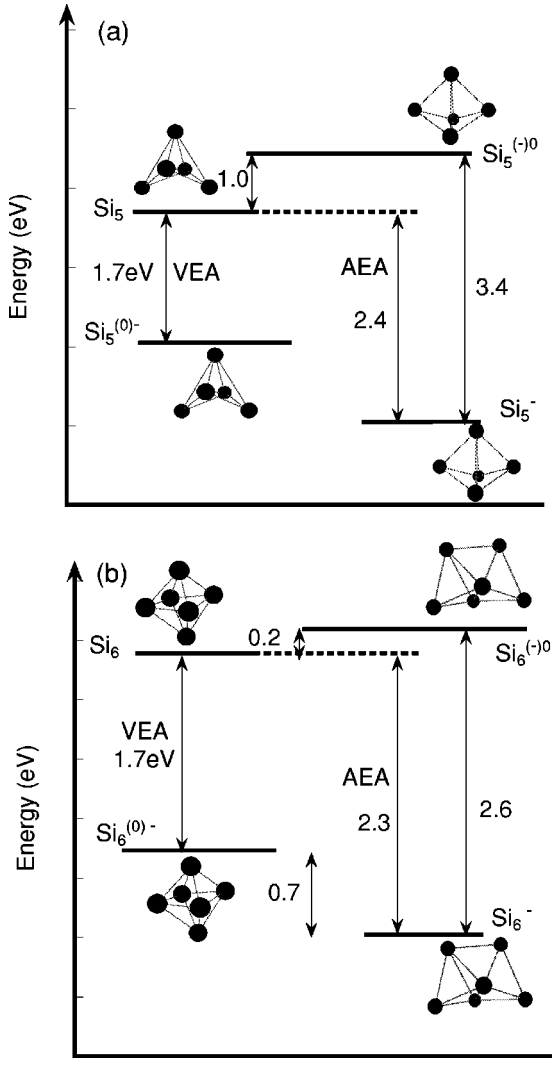


FIG. 2. Total-energy difference between the anions and neutral clusters for pentamer (a) and hexamer (b), employing the different geometries optimized with neutral or negatively charged condition. These values are calculated within the B3PW91 exchange-correlation functional. VEA (AEA) denotes vertical (adiabatic) electron affinity. Note that bicapped tetrahedron is more stable than distorted octahedron in anions of hexamer.

$Si_4^-$ is quite similar to the neutral one. However, for pentamer and hexamer, the most stable structures of anions have significant relaxation from the neutral ones. As pointed out first by Binggeli and Chelikowsky,[5] the trigonal bipyramid of $Si_5$ becomes elongated such that the apex to apex bond length of the pentamer changes significantly by about 10% in $Si_5^-$. The results of our calculations agree with theirs. For the hexamer, we found that $Si_6$ has an octahedral structure while $Si_6^-$ is either a bicapped tetrahedron or a distorted octahedron, which are energetically almost degenerate (within 0.2 meV).

The second part of the calculation is based on the GWA. Here we exploited the all-electron mixed-basis approach, where the one-particle wave function is represented by plane waves (PW's) and atomic orbitals to take into account both the core electron states and the empty free-electron-like states accurately. This approach has been applied successfully to various problems.[9,11] In previous papers,[9] some of the present authors have succeeded in determining the absolute values of the GWA quasiparticle energies of alkali-metal clusters by using this approach.

In the GWA, the one-electron self-energy $\Sigma(\omega)$ is given by (apart from the Hartree potential)[6–8]

$$\Sigma(\omega)=\frac{i}{2\pi}\int G(\omega+\omega')W(\omega')e^{i\eta\omega'}d\omega', \qquad (1)$$

where $G$ and $W$ denote, respectively, the one-particle Green's function and the dynamically screened Coulomb interaction; and $\eta$ is a positive infinitesimal number. The Fock exchange part of the self-energy, $\Sigma_x$, is obtained by replacing $W$ with the bare Coulomb interaction in Eq. (1), while we call $\Sigma_c=\Sigma-\Sigma_x$ the correlation part.

In the present study, we use the local-density-approximation (LDA) wave functions and eigenvalues to evaluate $G$ and $W$ from the viewpoint of the perturbation theory. The GWA quasiparticle energy is then given by

$$E_i^{\mathrm{GWA}}=E_i^{\mathrm{LDA}}+\frac{1}{1-(\partial\Sigma(\omega)/\partial\omega)_{E_i^{\mathrm{LDA}}}}\langle i|\Sigma(E_i^{\mathrm{LDA}})-\mu_{\mathrm{xc}}^{\mathrm{LDA}}|i\rangle, \qquad (2)$$

where $E_i^{\mathrm{LDA}}$ and $\mu_{\mathrm{xc}}^{\mathrm{LDA}}$ are the LDA eigenvalue and the exchange-correlation potential, respectively. Equation (2) has been widely used in the literature and is known to give good quasiparticle energies for moderately correlated electron systems.[11] Recently, it was claimed in Refs. 3 and 9 that Eq. (2) does not always give reliable quasiparticle energies when an energy level $i$, to be calculated, is positive or has a negative value that is close to the bottom of the continuum level $(E=0)$ because one cannot ignore interaction with the continuum states. That is, one needs to calculate the off-diagonal elements of $\Sigma-\mu_{\mathrm{xc}}^{\mathrm{LDA}}$ and then diagonalize this matrix to obtain accurate quasiparticle energies. In the present study, however, we focus on the lowest (highest) unoccupied (occupied) energies of the clusters which are far from the continuum level (see results). Because of this, to a very good approximation one can use Eq. (2) instead of the full Dyson equation.

We use a fcc supercell with a cubic edge of 20 Å. This is large enough to make interactions between the clusters negligible. We introduce the spherical cutoff of the Coulomb potential.[9,12] The cutoff energy for the PW's is taken to be 5 and 4 Ry for the calculations of the LDA wave functions and $\Sigma_c$, respectively. In the evaluation of $\Sigma_c$, we adopt the generalized plasmon-pole (GPP) model[7] and use 600 empty levels, corresponding to 10 eV in the calculations. The GPP model reproduces the experimental quasiparticle energies well.[7–9] The core contribution is ignored in $\Sigma_c$. On the other hand, for the evaluation of $\Sigma_x$ in the Fourier space, we use the cutoff energy of 14 Ry to take into account the core contribution. The core contribution to $\Sigma_x$ is very important and is considered fully in the calculations. We have carefully checked that all contributions are well converged with these cutoff energies and the number of empty levels within the

TABLE I. Contributions to the GWA quasiparticle energies (in eV) for the HOMO, and LUMO levels of silicon clusters and the experimental ionization potentials (Ref. 13) and vertical electron affinities (Refs. 14 and 15) with minus signs ($E_i^{\text{expt.}}$). $\mu_{\text{xc},i}^{\text{LDA}}=\langle i|\mu_{\text{xc}}^{\text{LDA}}|i\rangle$, $\Sigma_{\text{x},i}=\langle i|\Sigma_{\text{x}}|i\rangle$, and $\Sigma_{\text{c},i}(E_i^{\text{LDA}})=\langle i|\Sigma_{\text{c}}(E_i^{\text{LDA}})|i\rangle$ are the expectation values of, respectively, the LDA exchange-correlation potential, and the exchange part and the correlation part of the self-energy $\Sigma$. The final result $E_i^{\text{GWA}}$ is evaluated through Eq. (2). In the first column, $\text{Si}_n$ and $\text{Si}_n^{(-)0}$ denote neutral clusters with the geometry optimized under neutral and negatively charged conditions, respectively. Here, a bicapped tetrahedron is assumed for $\text{Si}_6^{(-)0}$. The experimental vertical EA's were read from the figures in Refs. 14 and 15.

| | | $E_i^{\text{LDA}}$ | $\mu_{\text{xc},i}^{\text{LDA}}$ | $\Sigma_{\text{x},i}$ | $\Sigma_{\text{c},i}(E_i^{\text{LDA}})$ | $E_i^{\text{GWA}}$ | $E_i^{\text{expt.}}$ |
|---|---|---|---|---|---|---|---|
| $\text{Si}_4$ | HOMO | −5.56 | −11.51 | −14.07 | +0.41 | −7.42 | −7.5 [a] |
| | LUMO | −4.50 | −9.59 | −5.63 | −0.96 | −1.92 | −2.0 [c] (−1.8 [b]) |
| $\text{Si}_5$ | HOMO | −5.86 | −10.83 | −12.71 | −0.06 | −7.57 | −7.8 [a] |
| | LUMO | −3.82 | −10.79 | −7.27 | −0.50 | −1.17 | |
| $\text{Si}_5^{(-)0}$ | HOMO | −5.48 | −10.57 | −12.88 | −0.05 | −7.83 | −7.8 [a] |
| | LUMO | −5.12 | −10.84 | −7.86 | −0.48 | −2.90 | −2.5∼−3.5 [b, c] |
| $\text{Si}_6$ | HOMO | −5.59 | −11.43 | −14.54 | +0.43 | −7.57 | −7.7[a] |
| | LUMO | −3.39 | −10.66 | −7.63 | −0.63 | −1.25 | |
| $\text{Si}_6^{(-)0}$ | HOMO | −5.59 | −11.37 | −14.25 | +0.36 | −7.77 | −7.7[a] |
| | LUMO | −4.57 | −10.86 | −7.98 | −0.50 | −2.50 | −2.2∼−2.6 [b, c] |

[a]Reference 13.
[b]Reference 14.
[c]Reference 15.

accuracy of 0.1 eV. Other technical details of the present calculations are explained in Ref. 9.

In Table I, we show the GWA quasiparticle energies $E_i^{\text{GWA}}$ for the HOMO (highest occupied molecular orbital) and the LUMO (lowest unoccupied molecular orbital) levels, as well as the experimental IP (Ref. 13) and EA (Refs. 14 and 15) with minus signs, $E_i^{\text{expt}}$. The absolute values of the quasiparticle energies for the HOMO and LUMO levels represent, respectively, the IP and the EA. Table I lists also different contributions to $E_i^{\text{GWA}}$ in Eq. (2). In the first column, symbols $\text{Si}_4$, $\text{Si}_5$, and $\text{Si}_6$ denote neutral clusters with the most stable ground-state geometry, while $\text{Si}_5^{(-)0}$ and $\text{Si}_6^{(-)0}$ denote also neutral clusters but those with the optimized geometry of anions. Here, the results for $\text{Si}_4^{(-)0}$ are not displayed because the neutral and negatively charged tetramers have nearly the same geometry and the same results.

For the HOMO levels of all the clusters studied here, the GWA quasiparticle energies $E_i^{\text{GWA}}$ agree well with the experimental IP's (Ref. 13) with minus signs ($E_i^{\text{expt.}}$), although the corresponding LDA eigenvalues ($E_i^{\text{LDA}}$) always deviate from the experimental values by about 2 eV. Comparing the results for the HOMO levels of $\text{Si}_n$ and $\text{Si}_n^{(-)0}$, one can see that the IPs are not so sensitive to the cluster geometry (see below). Also for the LUMO level of $\text{Si}_4$, the GWA quasiparticle energy agrees well with the experimental EA with minus sign. This is within the 0.1 eV error bar of the present calculation. This agreement can be attributed to the fact that the structures of $\text{Si}_4$ and $\text{Si}_4^-$ are quite similar. In contrast, for the LUMO levels of pentamer and hexamer, the quasiparticle energies depend strongly on the cluster geometry, reflecting that the structures are largely different between $\text{Si}_5$ and $\text{Si}_5^-$ and between $\text{Si}_6$ and $\text{Si}_6^-$. LUMO energy of $\text{Si}_n^{(-)0}$ is lower than that of $\text{Si}_n$, which is true already at the LDA level. There are two isomers of $\text{Si}_6^-$. We have repeated the same calculation also for the distorted octahedron. $E_i^{\text{GWA}}$ of the LUMO level of distorted octahedron becomes 0.2 eV deeper than that of the bicapped tetrahedron.

Let us now briefly explain the experimental process of measuring the EA. First, to separate the clusters by the time-of-flight mass spectroscopy, each cluster is charged up with one electron. Second, the photoelectron spectrum is observed by removing one electron *from the negatively charged cluster*. Then, the threshold and the first peak of the photoelectron spectrum are interpreted, respectively, as the vertical and adiabatic EA's *of a neutral cluster*. This experimental vertical EA is, then, generally different from the vertical EA in the inverse process which adds one electron to a neutral cluster. In fact, the structural change between the neutral and negatively charged clusters is so large in $\text{Si}_5$ and $\text{Si}_6$ that one cannot ignore this difference. The LUMO $E_i^{\text{GWA}}$ of $\text{Si}_n^{(-)0}$ and LUMO of $\text{Si}_n$ correspond, respectively, to the vertical EAs in the experimental photoemission process and in its inverse process. The resulting LUMO values are significantly different with 1.73 eV difference between $\text{Si}_5^{(-)0}$ and $\text{Si}_5$ and 1.25 eV difference between $\text{Si}_6^{(-)0}$ and $\text{Si}_6$, indicating clearly the breakdown of the time-reversal symmetry for photoemission and its inverse process. The values of $\text{Si}_5^{(-)0}$ and $\text{Si}_6^{(-)0}$ agree well with the experimental vertical EA's with minus signs ($E_i^{\text{expt.}}$ in Table I).

In order to obtain the adiabatic EA, the effect of the ionic relaxation during the photoemission process should be considered. The LUMO quasiparticle energy of $\text{Si}_n^{(-)0}$ can be corrected by the total-energy difference $\Delta E=E(\text{Si}_n^{(-)0})-E(\text{Si}_n^{(-)})$ between two neutral systems $\text{Si}_n^{(-)0}$ and $\text{Si}_n^{(-)}$ to yield the adiabatic EA with minus sign. Similarly the LUMO of $\text{Si}_n$ can be corrected by the total-energy difference $\Delta E$

TABLE II. Correction to the quasiparticle energies due to ionic relaxation during the photoemission process. The GWA quasiparticle energies $E_i^{\mathrm{GWA}}$ for the LUMO levels of $Si_n$ and $Si_n^{(-)}$ ($n=5,6$) can be corrected, respectively, by the total-energy differences, $\Delta E = E(Si_n^{(-)0}) - E(Si_n^{(-)})$ and $\Delta E = E(Si_n^{-}) - E(Si_n^{(0)-})$ to yield $E_i^{\mathrm{GWA}'}$ which should be compared with the experimental adiabatic EA (Ref. 15) with minus sign ($E_i^{\mathrm{expt.}}$). The values inside the parenthesos are from Ref. 14. All values are given in eV.

| | $E_i^{\mathrm{GWA}}$ | $\Delta E$ | $E_i^{\mathrm{GWA}'}$ | $E_i^{\mathrm{expt.}}$ |
|---|---|---|---|---|
| $Si_5$ | −1.17 | −0.96 | −2.13 | −2.3(−2.5) |
| $Si_5^{(-)}$ | −2.90 | +0.75 | −2.15 | −2.3(−2.5) |
| $Si_6$ | −1.25 | −0.71 | −1.96 | −2.2(−1.8) |
| $Si_6^{(-)}$ | −2.50 | +0.21 | −2.29 | −2.2(−1.8) |

$= E(Si_n^{-}) - E(Si_n^{(0)-})$ between an optimized negatively charged cluster $Si_n^{-}$ and a negatively charged cluster but with the neutral geometry ($Si_n^{(0)-}$). The relevant total energies and the corrections are listed in Tables II and III. In Fig. 2, we also show the total-energy diagram employing different geometries with charged and neutral conditions. Note that all the values shown in the diagram are evaluated within the B3PW91 functional. From Table II, one can see that excellent agreement (within 0.1∼0.2-eV error) is achieved between the present theory and the experimental adiabatic EA, reflecting that the time-reversal symmetry exists for the adiabatic EA. Nearly the same result can be obtained by starting from the two different calculations of $Si_n$ and $Si_n^{(-)}$ if the energy changes due to structural relaxations are properly accounted. Note that the LUMO energy of the distorted octahedron of $Si_6^{(-)}$ is slightly more negative than that of the bicapped tetrahedron. Therefore, it may be difficult to identify this in the photoemission spectra, as the emission from this may be hidden under the peak coming from the tetrahedral isomer.

Let us discuss that although the LUMO energy changes very much if one adds one electron to the neutral system, the HOMO energy does not change significantly (see Table I). We show the wave functions of the lowest (highest) unoccupied (occupied)level in Fig. 3 for both (a) $Si_5$ and (b) $Si_5^{(-)0}$. One can see that although the shape of the HOMOs is of course different from each other, but nature of bonding is nearly the same. Hence, the HOMO energy does not change so much. On the contrary, there is a dramatic change for the LUMO levels. That is, because of the geometrical change between $Si_5$ and $Si_5^{(0)-}$, the character of the LUMO state changed from one to another. Therefore, the LUMO energy changes very much.

In summary, the all-electron *GW* code using the plane waves and atomic orbitals as a basis set has been applied to

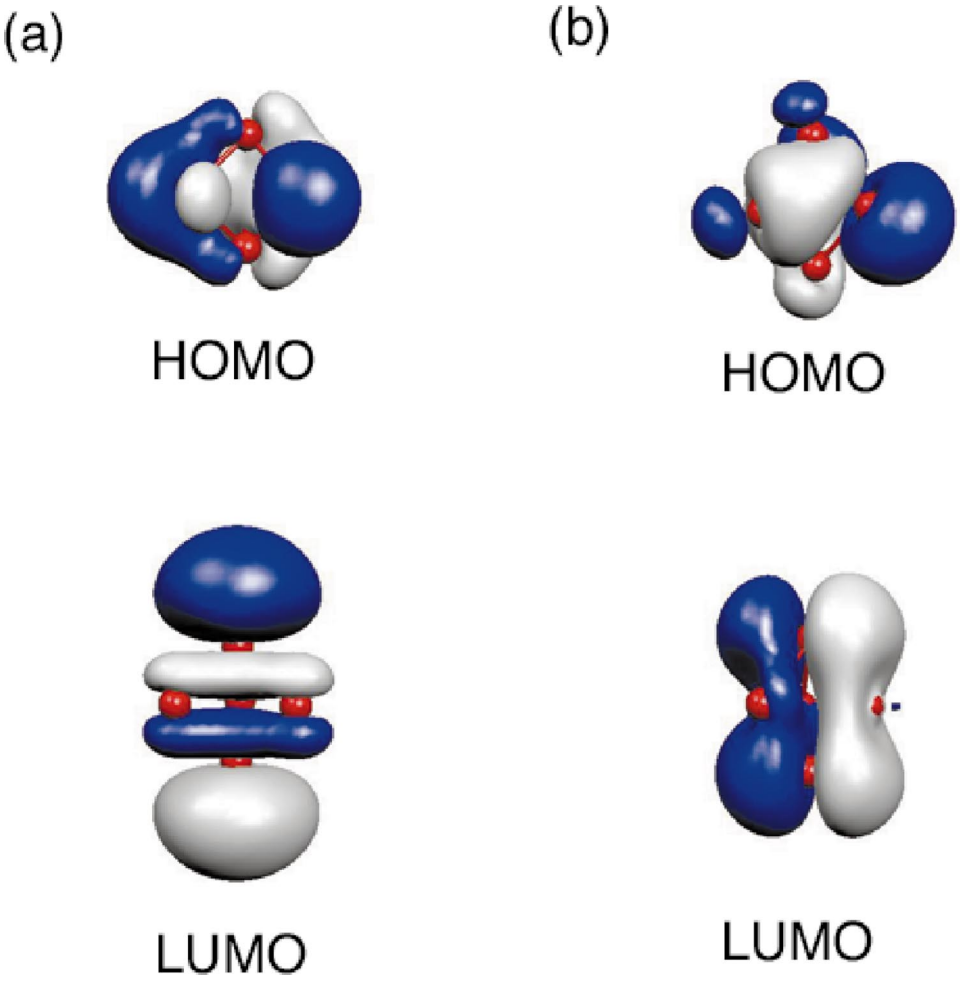


FIG. 3. (Color) The HOMO (LUMO) wave function of $Si_5$ and $Si_5^{(0)-}$. The characters of the LUMO state of $Si_5$ and $Si_5^{(0)-}$ are very different.

TABLE III. Total energies of the pentamer and hexamer employing different geometries with charged and neutral conditions (See also Fig. 2). All values are given in eV.

| | | Condition for the geometrical optimization | |
|---|---|---|---|
| Ionicity | $\Delta E$ | Neutral | Negative |
| Neutral | $+0.75$ | $Si_5$ $-39365.32$ | $Si_5^{(-)0}$ $-39364.57$ |
| Negative | $-0.96$ | $Si_5^{(0)-}$ $-39366.98$ | $Si_5^-$ $-39367.95$ |
| Neutral | $+0.21$ | $Si_6$ $-47239.62$ | $Si_6^{(-)0}$ $-47239.41$ |
| Negative | $-0.71$ | $Si_6^{(0)-}$ $-47241.27$ | $Si_6^-$ $-47241.96$ |

small silicon clusters. The resulting GWA quasiparticle energies for the HOMO levels are in good agreement with the experimental IP's for all clusters studied here, while the GWA quasiparticle energies for the LUMO levels are in excellent agreement with the experimental vertical EA's, in particular, for $Si_4$ in which the structural change between the neutral and charged clusters is very small. The structures of $Si_5$ and $Si_6$ change significantly if the systems are negatively charged. This affects the GWA quasiparticle energies very much, in particular, for the LUMO levels. In this paper, we have manifested, that the time-reversal symmetry is strongly violated between the experimental photoemission process and its inverse process. In fact, the vertical EA's are significantly different between these two processes. On the other hand, the effect of the ion relaxation becomes important in the adiabatic EAs, for which the time-reversal symmetry holds accurately (i.e., the energies evaluated in the forward and backward processes are the same within the error bar). The corresponding GWA results are in excellent agreement with the recent experimental EA's (Ref. 15) when the necessary energetic correction is taken into account. A more concrete description of the method as well as the results for the higher quasiparticle energies (including also the imaginary parts relating to the lifetime of quasiparticles) will be reported elsewhere. It is highly desirable in the future that similar systematic studies be performed for other clusters.

The authors thank the Center for Computational Materials Science of the Institute for Materials Research, Tohoku University for the support of the SR8000 supercomputing facilities. V.K. gratefully acknowledges the hospitality at the Institute for Materials Research and the support from JSPS. One of the authors (S.I.) thanks Special Coordination Funds for Promoting Science and Technology from the Ministry of Education, Culture, Sports, Science, and Technology of the Japanese government.

[1] J.C. Grossman and L. Mitas, Phys. Rev. Lett. **74**, 1323 (1995).
[2] F. Kootstra, P.L. de Boeij, and J.G Snijders, Phys. Rev. B **62**, 7071 (2000).
[3] J.C. Grossman, M. Rohlfing, L. Mitas, S.G. Louie, and M.L. Cohen, Phys. Rev. Lett. **86**, 472 (2001).
[4] I. Vasiliev, S. Öǔt, and J.R. Chelikowsky, Phys. Rev. Lett. **86**, 1813 (2001).
[5] N. Binggeli and J.R. Chelikowsky, Phys. Rev. Lett. **75**, 493 (1995).
[6] L. Hedin, Phys. Rev. **139**, A796 (1965).
[7] M.S. Hybertsen and S.G. Louie, Phys. Rev. Lett. **55**, 1418 (1985).
[8] R.W. Godby, M. Schlüter, and L.J. Sham, Phys. Rev. Lett. **56**, 2415 (1986).
[9] S. Ishii, K. Ohno, Y. Kawazoe, and S.G. Louie, Phys. Rev. B **63**, 155104 (2001); **65**, 245109 (2002).
[10] Final *GW* quasiparticle energies do not depend on the type of exchange-correlation potential and therefore the strict atomic configurations significantly.
[11] See, for example, K. Ohno, K. Esfarjani, and Y. Kawazoe, *Computational Materials Science*, Solid-State Sciences Vol. 129 (Springer-Verlag, Berlin, Heidelberg 1999); and references therein.
[12] G. Onida, L. Reining, R.W. Godby, R.D. Sole, and W. Andreoni, Phys. Rev. Lett. **75**, 818 (1995).
[13] K. Fuke, K. Tsukamoto, and F. Misaizu, Z. Phys. D: At., Mol. Clusters **26**, S204 (1993).
[14] O. Cheshnovsky, S.H. Yang, C.L. Pettiette, M.J. Craycraft, Y. Liu, and R.E. Smalley, Chem. Phys. Lett. **138**, 119 (1987).
[15] M. Maus, G. Gantefor, and W. Eberhardt, Appl. Phys. A: Mater. Sci. Process. **70**, 535 (2000).